The Thesis Committee for Sunil Kishor Prajapati
Certifies that this is the approved version of the following Thesis:

Comparison of Muscle Coordination Between Individuals Post-Stroke and Kinematically Constrained Walking

APPROVED BY
SUPERVISING COMMITTEE:

James S. Sulzer, Supervisor

Richard R. Neptune

Comparison of Muscle Coordination Between Individuals Post-Stroke and Kinematically Constrained Walking

by

Sunil Kishor Prajapati

Thesis

Presented to the Faculty of the Graduate School of

The University of Texas at Austin

in Partial Fulfillment

of the Requirements

for the Degree of

Master of Science in Engineering

The University of Texas at Austin

May 2019

Dedication

This thesis is dedicated to my parents, Kishor and Daxa Prajapati, my sister, Purvi Prajapati and my friends who have all taught me invaluable lessons about life, friendship and love.

Acknowledgements

I would first like to show my appreciation and thanks to my advisor, Dr. James Sulzer, not only for his guidance throughout my graduate tenure but also for his patience, willingness to assist me in any manner and constant support. There is no doubt in my mind he has helped me grow as an engineer, a researcher and as a person, I am truly grateful to have been a part of his lab in both my undergraduate and graduate terms. I owe many thanks to Tunc Akbas for taking me under his wing when I first joined the Rewire lab. He served as a wonderful role model and someone I truly aspire to be like. I would also like to thank Dr. Rick Neptune for serving on my committee, being an individual I could approach whenever I had any issue or concerns and providing a wide pool of knowledge, experience and insight. Thank you to Jay and Otto for allowing me to rant to them. Finally, I would like to thank my parents and my sister for their continuous support throughout my educational journey, without their support, I would not be where I am today.

Abstract

Comparison of Muscle Coordination Between Individuals Post-Stroke and Kinematically Constrained Walking

Sunil Kishor Prajapati, M.S.E.

The University of Texas at Austin, 2019

Supervisor: James S. Sulzer

Abnormal motor coordination affects motor function following stroke, yet we lack a complete characterization of how such abnormal coordination affects movements such as gait. Previous research found that post-stroke gait exhibited fewer movement primitives, or muscle modules, than healthy individuals, suggesting abnormal coordination may affect gait function. However, aside from abnormal coordination, the reduced number of modules could also be due to compensations in response to other impairments such as increased muscle tone and spasticity. Our previous research compared gait in those with post-stroke Stiff-Knee Gait (SKG) to healthy individuals with kinematically constrained knee flexion. While healthy individuals compensated with pelvic obliquity, those with post-stroke SKG also exhibited greater hip abduction, suggesting the motion may be related to neural impairments such as abnormal coordination. We hypothesize that abnormal coordination, not the compensations due to restricted ranges of motion induced by other impairments, is associated with reduced gait function. In this experiment, we compared muscle coordination patterns emerging from healthy individuals with and without restricted knee

kinematics to a cohort of individuals post-stroke, both with and without SKG. We predicted the number of muscle modules would be fewer than healthy individuals with similar gait kinematics and found that mechanical knee restriction reduced the number of modules similar to those with post-stroke SKG in walking. Constraining healthy motions resulted in similar muscular coordination patterns to unrestricted gait suggesting the robustness of muscle recruitment despite a kinematic perturbation. The composition of modules in the pre-swing phase between those with SKG and the mechanically restricted group differed (Spearman's ρ = -0.024), whereas comparisons between post-stroke individuals without SKG (NSKG) and the healthy group were similar (Spearman's ρ = 0.833). We found those with SKG relied less on hamstrings than healthy counterparts, suggesting an altered motor command beyond adaptation. Muscle coordination patterns in constrained motions during gait were not similar to SKG while the NSKG group showed greater similarity to normal walking. Thus, our data suggests that abnormal coordination may play a greater role in SKG than those without SKG. The results of this comparison will help develop more accurate interventions for clinical treatment.

Table of Contents

List of Tables

List of Figures

Chapter 1: Introduction

Stroke is the leading cause of long-term disability and causes numerous impairments such as muscle weakness, spasticity, abnormal muscle coordination and altered proprioception leading to gait disorders (Benjamin et al., 2018; Bobath, 1999; Kerrigan et al., 1991; Watkins et al., 2002). Stiff-Knee Gait (SKG) is a common disorder following a stroke which results in reduced knee flexion during the swing phase on the paretic side. As a result of this reduced knee flexion, studies have suggested post-stroke SKG individuals compensate by increasing hip circumduction, hip hiking, and/or vaulting (i.e. contralateral heel rise) (Kerrigan et al., 2000, 1991; Perry et al., 1992).

In addition to compensations to altered gait mechanics, abnormal muscle coordination occurring after stroke may also lead to gait deviations. Changes in lower limb coordination during non-gait events has been well-documented (Cruz et al., 2009; Cruz and Dhaher, 2008; Finley et al., 2008). However, we lack characterization as to how this abnormality affects post-stroke gait. The underlying motor coordination patterns can be characterized from measurements of electromyography (EMG) data of multiple muscles (Safavynia et al., 2011). For example, non-negative matrix factorization (NNMF) has been used extensively to extract a modular set of coordination patterns to describe the motor function of an individual (Barroso et al., 2017; Routson et al., 2013; Ting and Macpherson, 2005). The greater the number of muscle modules, or coordination patterns, the greater the level of coordination. For example, NNMF was used to determine that people post-stroke exhibited fewer muscle modules than healthy age-matched individuals, suggesting that stroke reduces muscle coordination which adversely affects gait performance (Clark et al., 2010).

While abnormal muscle coordination is common after stroke, it is unclear how it manifests itself in post-stroke SKG. SKG has been traditionally believed to be caused by overactivity of the rectus femoris, contributing to reduced knee flexion in individuals post-stroke (Reinbolt et al., 2008; Thawrani et al., 2012). In response, clinical studies have suggested that the reduced knee flexion is compensated by greater hip circumduction (Perry et al., 1992). However, in a study where a robotic actuator was applied to individuals with post-stroke SKG to increase knee flexion, they observed a biomechanically unnecessary increase in hip circumduction (Sulzer et al., 2010). Further descriptive analysis with musculoskeletal modeling and simulation revealed an abnormal coordination pattern between rectus femoris and gluteus medius (Akbas et al., 2019a). In this study, a musculoskeletal simulation of individuals with post-stroke SKG were prescribed with a robotic perturbation during the pre-swing phase to generate sufficient knee flexion (Akbas et al., 2019a). In previous work, we restricted knee flexion in healthy individuals using a commercial knee brace to simulate post-stroke SKG knee kinematics in order to observe resulting compensations (Akbas et al., 2019b) and found that reduced knee flexion did not change hip motion but increased pelvic obliquity (i.e. hip hiking; Figure 1). As such, hip circumduction does not appear as a compensation for reduced knee flexion, but instead may be part of an abnormal coordination pattern. The difference in muscle coordination patterns between people with post-stroke SKG and those compensating to mechanical knee restriction is unknown. Delineating compensation from abnormal coordination can assist in creating robotic interventions based on muscle coordination patterns which may develop more accurate treatment regimens than currently available.

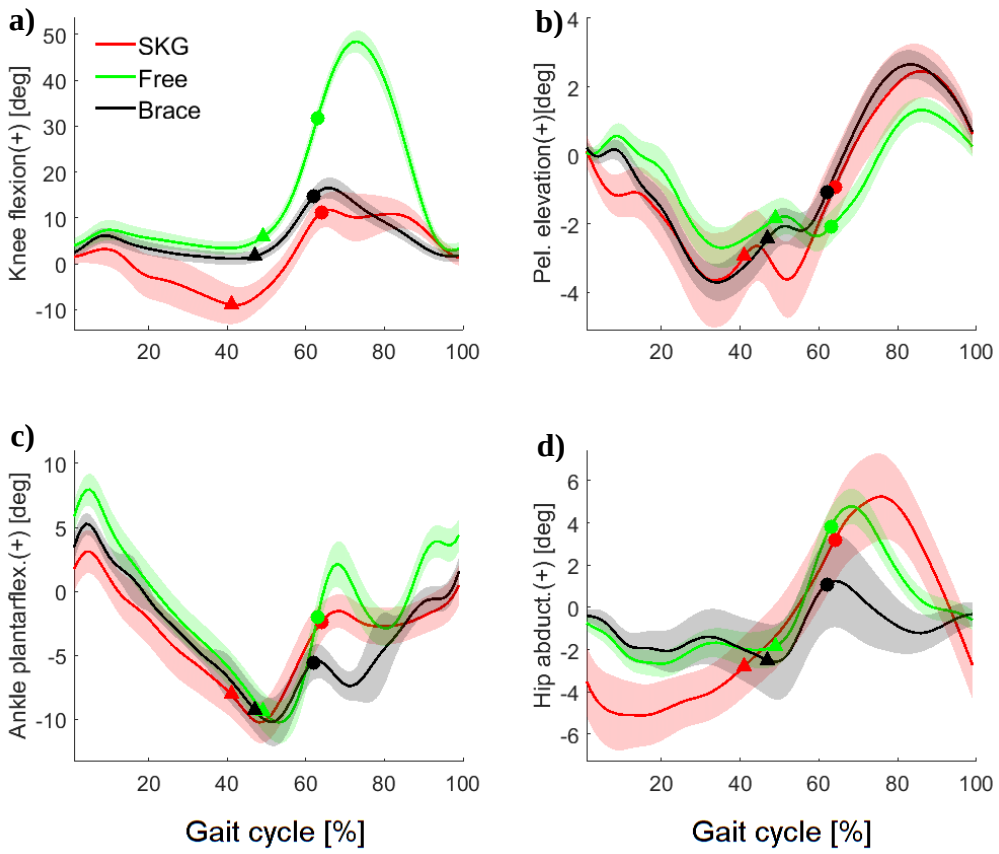

Figure 1: The knee flexion (a), pelvic elevation (b), ankle plantarflexion (c) and hip abduction (d) angles for the constrained sided for healthy individuals and speed-matched post-stroke SKG subjects from our previous study. The standard errors are shown by the shaded regions. Contralateral heel strike (triangles) and ipsilateral toe-off (circles) are denoted on each of the graphs. We found that despite similar knee flexion between the *Brace* and *SKG* groups, there was a reduction in hip abduction by the healthy *Brace* group while *SKG* group increased abduction.

The goal of this study was to examine the muscle coordination patterns associated with kinematically constrained knee flexion in pre-swing phase compared to post-stroke SKG. We analyzed the muscle coordination patterns from healthy individuals with and without restricted kinematics and compared those to a cohort of post-stroke individuals both with varying degrees of knee flexion. The muscle coordination differences between healthy individuals with knee restriction and those with SKG would reveal different neural control strategies during pre-swing in response to similar gait kinematics. We hypothesized that muscles associated with compensatory actions such as ankle dorsiflexion and hip hiking would be active in unimpaired individuals when knee flexion is restricted, whereas muscles associated with abnormal coordination (e.g. gluteus medius) will be associated with post-stroke SKG. We also expected to see a decrease in the number of coordination patterns as a result of the kinematic restriction, and an even greater reduction in the post-stroke SKG population. Previous simulation work suggests modules are organized around biomechanical function, therefore, by altering the kinematics, we change the basic biomechanical function needed to create a well-coordinated movement (Neptune et al., 2009). Understanding the origin of gait deviations will help promote targeted treatments. This study will provide motivation for future research in other neurological disorders which contribute to reduced motor function to provide recovery for individuals with neuromuscular impairment.

Chapter 2: Methods

EXPERIMENTAL DATA

We recruited 14 healthy participants (13 right-side dominant, 10 male, age 45±11) with no history of neuromuscular impairment gave written informed consent according to the Institutional Review Board of the University of Texas at Austin (Table A1). We applied a commercial knee brace (Comfortland Medical, Mebane, NC) to provide kinematic restriction to the left leg, allowing approximately 25° of knee flexion, a method shown to imitate SKG kinematics (Akbas et al., 2019b; Lewek et al., 2012). A 2x2 factorial design consisting of the factors of knee restriction and speed were used to carry through with this experiment resulting in four total conditions. The *Brace* condition consisted of the knee brace restriction with a range-of-motion setting at 0° nominally, while the *Free* condition was when no restriction was applied and subjects were fully able to flex their knees with the knee brace still attached. All conditions were conducted on a split-belt force treadmill (Bertec, Columbus OH). Each of the conditions were conducted for two minutes at two speeds, slow (0.5 m/s) and normal (1.0 m/s). The two speeds represented the average comfortable walking speed of individuals with post-stroke SKG (Sulzer et al., 2010) and healthy individuals, respectively. The order of the condition-walking speed pairs were randomized for each subject. Lower limb kinematic data were collected using inertial measurement units (Xsens, Eschende, Netherlands). EMG sensors (Delsys, Natick, MA) were attached to eight muscles to measure the muscle activity of the constrained limb throughout the different conditions. To reduce the impedance seen during muscle activity measurements due to dead skin cells, skin oil, moisture and hair, the area of interest was shaved and cleaned using isopropyl alcohol. The eight muscles incorporated in this study were Tibialis Anterior (TA), Soleus (SOL), Medial Gastrocnemius (GAS), Vastus Medialis

(VM), Rectus Femoris (RF), Medial Hamstring (MH), Lateral Hamstring (LH) and Gluteus Medius (GM). Each of the healthy participants walked for two minutes for each condition. The final one-third of each walking segment was observed so that adaptation to the knee brace could be accounted for.

Kinematic data was collected at 60 Hz, while force measurements from the treadmill and muscle excitation signals from surface electrodes (Bortec, Calgary, AB) were collected at 1 kHz. Knee flexion, ankle plantarflexion and hip abduction angles of the restricted (ipsilateral) and unrestricted (contralateral) limb were extracted from the final one-third of each trial. Pelvic obliquity, also known as hip hiking, was calculated by the coronal angle of the pelvis (Michaud et al., 2000). Range-of-motion (ROM) for each movement was defined between minimum and maximum joint angle measures in positive directions during pre-swing and swing phases of the gait cycle. Stance ratio was denoted as the ratio of stance phase of the opposing limbs (constrained/unconstrained) as means to assess gait symmetry between conditions and groups. Additionally, step length, the distance between two successive placements of the constrained foot and cadence, the steps per minute, were extracted to observe changes due to speed and restriction.

DISTINGUISHING POST-STROKE STIFF-KNEE GAIT

Additionally, data was previously collected by our collaborator, Dr. Steven Kautz from the Medical University of South Carolina, from 46 hemiparetic post-stroke individuals (18 left hemiparesis, 29 male, age: 57±14 years) walking on a split-belt instrumented treadmill (Bertec, Columbus, OH) at their self-selected speed (0.10 - 0.80 m/s) and anonymized (Tables A2-A3). Supplemental information regarding the subjects can be found in Brough et al. (2019). We classified post-stroke population as *SKG* if the ROM of the non-paretic limb exhibited ROM greater than 15° of the paretic limb due to

the various definitions regarding distinction of post-stroke SKG individuals (Campanini et al., 2013; Goldberg et al., 2006; Lelas et al., 2003; Reinbolt et al., 2008; Stoquart et al., 2008). A total of 18 subjects were classified as *SKG* from the dataset. The remaining subjects from this dataset (n = 28) were labeled non-SKG (*NSKG*). In order to confirm the speeds were not significantly different between the healthy and post-stroke groups, as these individuals could self-select their speed, a two-sample t-test was run. The results showed no significant difference in speed with healthy counterparts in either the *SKG* ($p = 0.2562$) and *NSKG* ($p = 0.7652$) groups.

ASSESSING MUSCLE ACTIVITY

Coordinated movements are controlled by the cerebellum, peripheral nerves of the body and the spine, however, it is very difficult to measure neural activity through movements. One method to quantify the neural activity is through muscle activity as it indicates the motoneuron activity and forces the brain attempts to achieve. However, because EMG data can be variable and large, we applied two methods to analyze the resulting muscle patterns, nonnegative matrix factorization (NNMF) and integrated EMG (iEMG).

NON-NEGATIVE MATRIX FACTORIZATION

The collected EMG data was processed and compared using two methods including techniques mentioned in Clark et al. (2010). The muscle activations were high-pass filtered at 40 Hz using a zero-lag 4^{th} order Butterworth filter, demeaned, rectified and low-pass filtered at 4 Hz using a zero-lag 4^{th} order Butterworth filter. Data was separated into gait cycles using left heel strikes for each participant corresponding to the given condition-speed pair. The heel-strike was detected using the instrumented split-belt treadmill based on a vertical force threshold of 20 N. The EMG from each muscle was normalized to its

peak value for each walking condition and resampled at each 1% of the gait cycle. The data for each subject and each condition was partitioned into an *m* x *t* matrix (EMG_O), where *m* corresponds to the number of muscles (8) and *t* is the total number of steps multiplied by 101 to represent the gait cycle (*t* = no. of steps x 101). Afterwards, the matrix was run through a NNMF algorithm (Lee and Seung, 1999; Ting and Macpherson, 2005) where *n*, the number of modules, is specified a priori. As a result, the NNMF determines the properties of the modules by producing two matrices: an *m* x *n* matrix, which specifies the relative weighting of each muscle within each module and an *n* x *t* matrix, which specifies the activation timing profiles of each module across the gait cycle. Once the two matrices are formed, they are then multiplied to create a reconstructed version of the original EMG signal (EMG_r). We made no *a priori* assumption about the numeric value of modules needed to reconstruct the EMG signals. Therefore, in order to determine the number of modules needed for EMG reconstruction separate NNMF analyses were performed with the number of modules varying from one to five, for each subject. To determine the minimum number of modules needed to sufficiently recreate the original EMG signal (EMG_O), we calculated the variability accounted for (VAF) using methods described by Clark et al. (2010). If VAF was $\geq$ 90% for each of the eight muscles, then it was determined that additional modules were not needed. Else, the number of modules assumed were increased until the addition of another module did not increase the VAF > 5% for the muscle with the lowest VAF. Individuals exhibit a greater number of modules if they are walking at speeds greater than their self-selected speed (Yokoyama et al., 2016). Therefore, to account for the possibility that multiple modules are potentially active during the pre-swing phase due to gait speed differences, the corresponding pre-swing module was extracted using a multifactorial method. The max, mean, integral and integral per unit

length were observed for the corresponding activation timing profiles to determine which modules were active within the 100 milliseconds prior to toe-off region of the gait cycle. Lastly, a co-contraction measure was calculated where the ratio of relative magnitudes between the quadriceps and hamstrings were taken to view whether contributions between each group showed similar quadriceps/hamstrings distribution.

INTEGRATED EMG

Integrated EMG (iEMG) combines the ability to observe temporal and spatial characteristics of muscle activity (Vance et al., 2004). Therefore, as an additional analysis to the comparison of module compositions, the filtered EMG signals were integrated from the pre-swing to toe-off phase, where the pre-swing phase was defined as 100 milliseconds prior to toe-off. This region is where post-stroke SKG individuals exhibited an abnormal coupling between the rectus femoris and gluteus medius following robotic perturbation (Akbas et al., 2019a). For this analysis, the muscle signals were normalized to the maximum of the muscle of all conditions. By normalizing to this factor, we can compare the four conditions within our experiment. However, if the same signals input into the NNMF algorithm were used, redundant results would be output as the outcomes would simply show relative contributions of each muscle, similar to what is exhibited in the modules. For this reason, the stroke group signals were not able to be used for the iEMG analysis as there was only one condition which was analyzed, therefore normalizing to the max of the condition would result in the same signal being put through iEMG and NNMF analysis. The iEMG activities for each of the muscles for each of the groups were averaged and used to confirm the results found from the module analysis.

STATISTICS

Comparisons of age and gait speed were done using two sample t-tests to determine significant differences between groups. To compare discrete module numbers between conditions, we used a Friedman's Rank ANOVA test followed by Wilcoxon-Rank Sum test. A Bonferroni-Holm correction for multiple comparisons was used for the Rank Sum tests (uncorrected $\alpha < 0.05$). Comparison of module composition and activation profiles were performed using Spearman and Pearson correlations, respectively. A linear mixed model with the subjects as random effects was used to compare the iEMG measures of the individual muscles as well as kinematic and spatiotemporal measures for the healthy and stroke populations. The linear mixed model was followed by a Tukey-Kramer *post hoc* test to evaluate the significance of the differences in the outcome variables between factors ($\alpha < 0.05$) followed by a Bonferroni-Holm correction for multiple comparisons.

Chapter 3: Results

COMPARISONS WITHIN HEALTHY INDIVIDUALS

KINEMATIC AND SPATIOTEMPORAL COMPARISONS

A summary of the outcome measures for joint angle ROM and spatiotemporal characteristics are given below (Table 1). The following highlights the statistical comparisons based on the linear mixed model and non-parametric tests for the respective analyses. The average trajectories for all of the aforementioned kinematic measures for all the subjects in *Free* and *Brace* for both walking speeds are shown in Figure 2.

We observed a main effect of knee restriction on ankle ROM ($F_{(1,41)} = 32.54$, $p < 0.001$) and knee flexion ROM ($F_{(1,41)} = 186.66$, $p < 0.001$ all which reduced in the *Brace* when compared to the *Free* condition. Hip abduction ($F_{(1,41)} = 0.204$, $p = 0.652$) and pelvic obliquity ($F_{(1,41)} = 0.0006$, $p = 0.980$) ROM did not show any significant trends due to the knee restriction. For the slow speed, pelvic obliquity ROM ($t = 3.301$, $p < 0.01$) increased for the *Brace* condition compared to the *Free* condition while knee ROM ($t = 13.23$, $p < 0.001$) and ankle ROM ($t = 13.23$, $p < 0.001$) increased in the *Free* condition when compared to the *Brace* condition. The normal walking speed conditions showed a significant decrease in knee ROM ($t = 13.23$, $p < 0.001$) and ankle ROM ($t = 12.95$, $p < 0.001$) compared to the *Brace* condition.

Other than knee ($F_{(1,41)} = 3.228$, $p = 0.072$) and pelvis ($F_{(1,41)} = 2.871$, $p = 0.0902$) ROM, which did not show significant changes due to speed, the hip ($F_{(1,41)} = 20.683$, $p < 0.001$) and ankle ($F_{(1,41)} = 19.059$, $p < 0.001$) exhibited greater ROM due to the faster walking speed. Within the *Brace* condition, we saw an increase in ankle ($t = 4.058$, $p < 0.001$), knee ($t = 5.589$, $p < 0.001$) and hip ($t = 3.793$, $p < 0.001$) ROM as the gait speed was changed from slow to normal. For the *Free* condition, the ankle ($t = 7.582$, $p < 0.001$),

knee (t = 6.991, p < 0.001) hip (t = 2.75, p < 0.05) and pelvic obliquity (t = 2.465, p < 0.05) ROM increased due to the increase in gait speed.

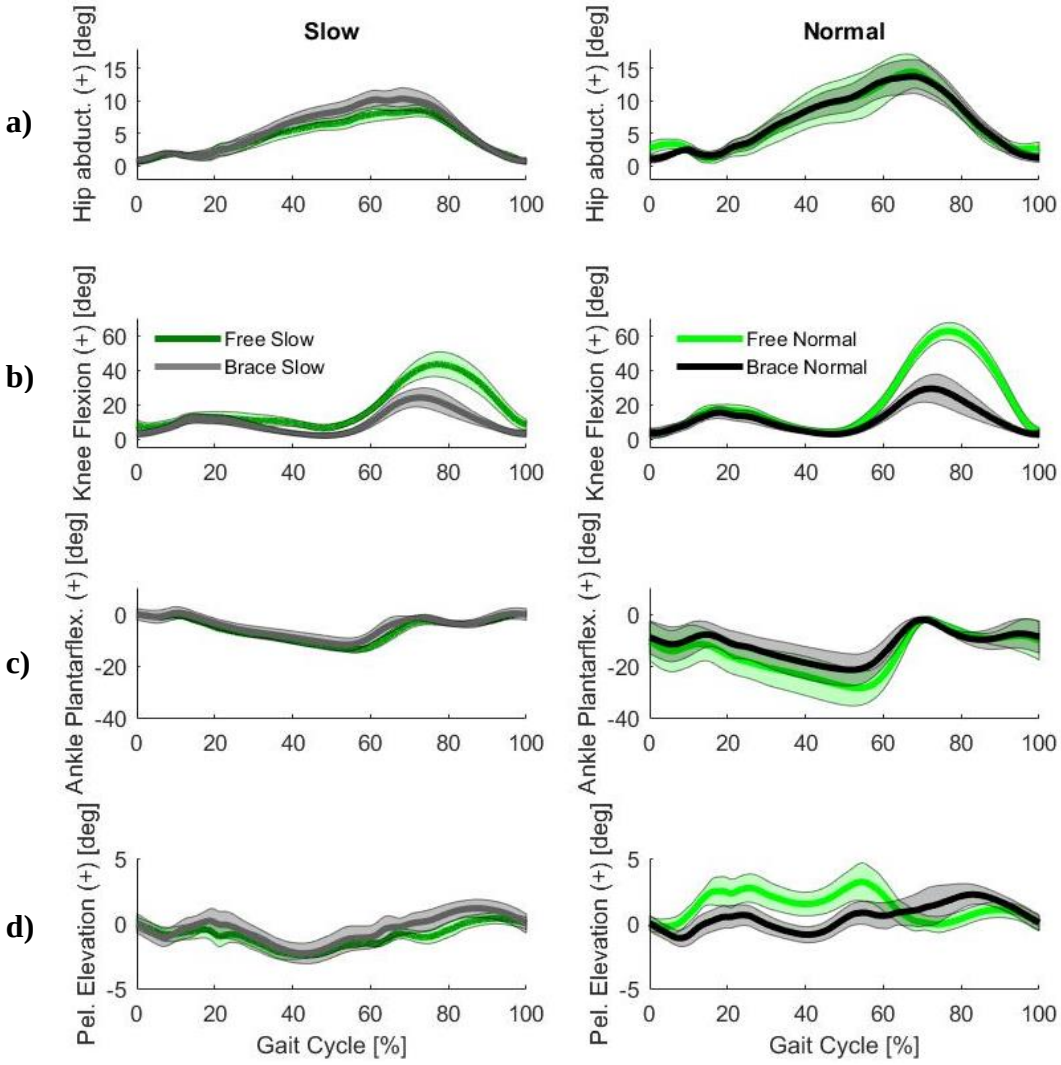

Figure 2: The hip abduction (a), knee flexion (b), ankle plantarflexion (c) and pelvic obliquity (d) angles for the constrained side under different conditions (*Brace* and *Free*) are given for slow and normal walking speeds

Table 1: Summary of the joint angle ROM and spatiotemporal gait measures for healthy gait with and without knee brace restriction. The measures display the mean values and standard deviations. The level of significance between *Free* and *Brace* for the slow condition are denoted as # $p < 0.05$, ## $p < 0.01$, ### $p < 0.001$; between *Free* and *Brace* for the normal walking speed conditions denoted as ¢ $p < 0.05$, ¢¢ $p < 0.01$, ¢¢¢ $p < 0.001$; between the two *Free* conditions denoted as: ‡ $p < 0.05$, ‡‡ $p < 0.01$, ‡‡‡ $p < 0.001$; between the two *Brace* conditions denoted as * $p < 0.05$, ** $p < 0.01$, *** $p < 0.001$.

Outcome Measures \ **Group**		**Free Slow**	**Brace Slow**	**Brace Normal**	**Free Normal**
Kinematic Measures	Knee ROM (°)	$51.5 \pm 9.85^{\#\#\#, ‡‡‡}$	$23.0 \pm 12.4^{***}$	$30.9 \pm 14.3^{¢¢¢}$	61.1 ± 9.00
	Hip abd. ROM (°)	$10.8 \pm 2.86^{‡‡}$	$11.6 \pm 4.12^{***}$	14.3 ± 5.60	14.3 ± 6.38
	Ankle ROM (°)	$23.7 \pm 12.2^{\#\#\#, ‡‡‡}$	$18.3 \pm 10.5^{***}$	$22.7 \pm 12.0^{¢¢¢}$	30.2 ± 13.2
	Pel obl. ROM (°)	$3.70 \pm 1.46^{\#\#, ‡}$	4.78 ± 1.22	4.52 ± 1.12	5.63 ± 2.96
Spatiotemporal	Stance Ratio	$0.98 \pm 0.02^{\#\#\#}$	0.95 ± 0.04	$0.94 \pm 0.05^{¢¢¢}$	0.98 ± 0.03
	Cadence	$107 \pm 9.78^{\#\#\#}$	93.0 ± 6.72	$99.0 \pm 15.1^{¢¢¢}$	107 ± 3.62
	Step Length	$0.36 \pm 0.07^{‡‡‡}$	$0.38 \pm 0.09^{***}$	0.57 ± 0.09	0.55 ± 0.09

QUANTITATIVE MODULE ANALYSIS

Within the healthy group, we found the number of modules decreased with the brace (Figure 3). The Friedman's rank ANOVA indicated that modules did not change with speed ($F_{(1,1)} = 0$, $p = 1$), which was used as a blocking factor, but did with knee restriction ($F_{(1,1)} = 4.5722$, $p < 0.05$). There was no interaction between speed and knee restriction on number of modules ($F_{(1,1)} = 1.8788$, $p = 0.176$).

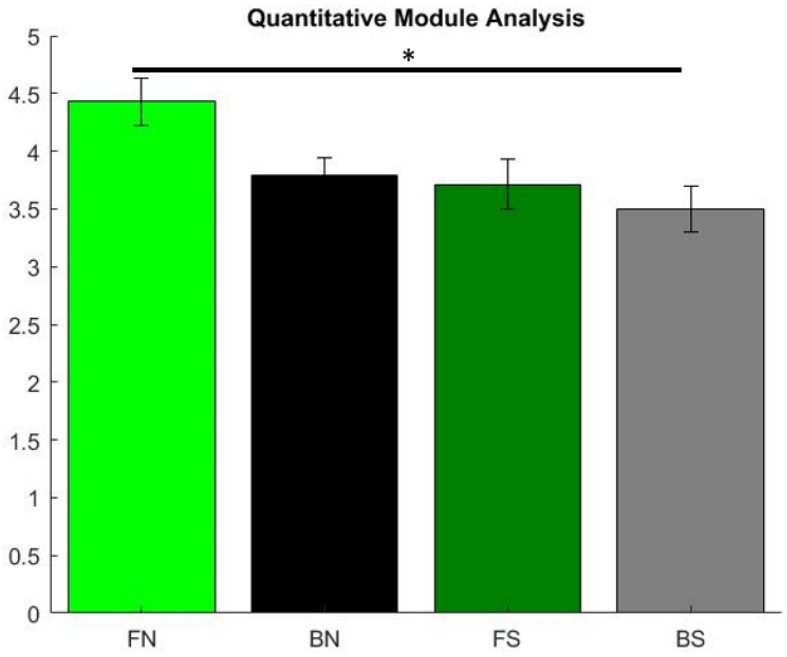

Figure 3: Average with standard error number of modules exhibited between healthy conditions for slow and normal walking speeds. The number of modules reduced as a result of the kinematic restriction, however, after the Bonferroni-Holm adjustment only *Free* Normal and *Brace* Slow showed difference ($p < 0.05$).

MODULE COMPOSITION

For the four conditions within the experiment, varying module compositions were extracted for the pre-swing phase (Figure 4). We also compared similarity of module compositions (Table 2). For the slow speed conditions, we found similar module compositions between the *Free* and *Brace* (Spearman's $\rho = 0.905$). However, at the normal walking speed, the two conditions were not as similar (Spearman's $\rho = 0.548$). Changes in gait speed show similar composition for the *Brace* condition (Spearman's $\rho = 0.929$) while the *Free* condition shows moderate similarity (Spearman's $\rho = 0.714$). The *Brace* slow and *Free* normal showed the poorest similarity (Spearman's $\rho = 0.476$). When the speed is changed for these two conditions, *Brace* normal and *Free* slow, the modular composition shows very strong correlations (Spearman's $\rho = 0.905$) between the two conditions. The co-contraction measures found greater use of the quadriceps for the normal speed. For the slow speed, the co-contraction measure for *Free* (1.14) and *Brace* (1.18) showed lower relative contributions from the quadriceps when compared to the normal speed *Free* (1.57) and *Brace* (1.51).

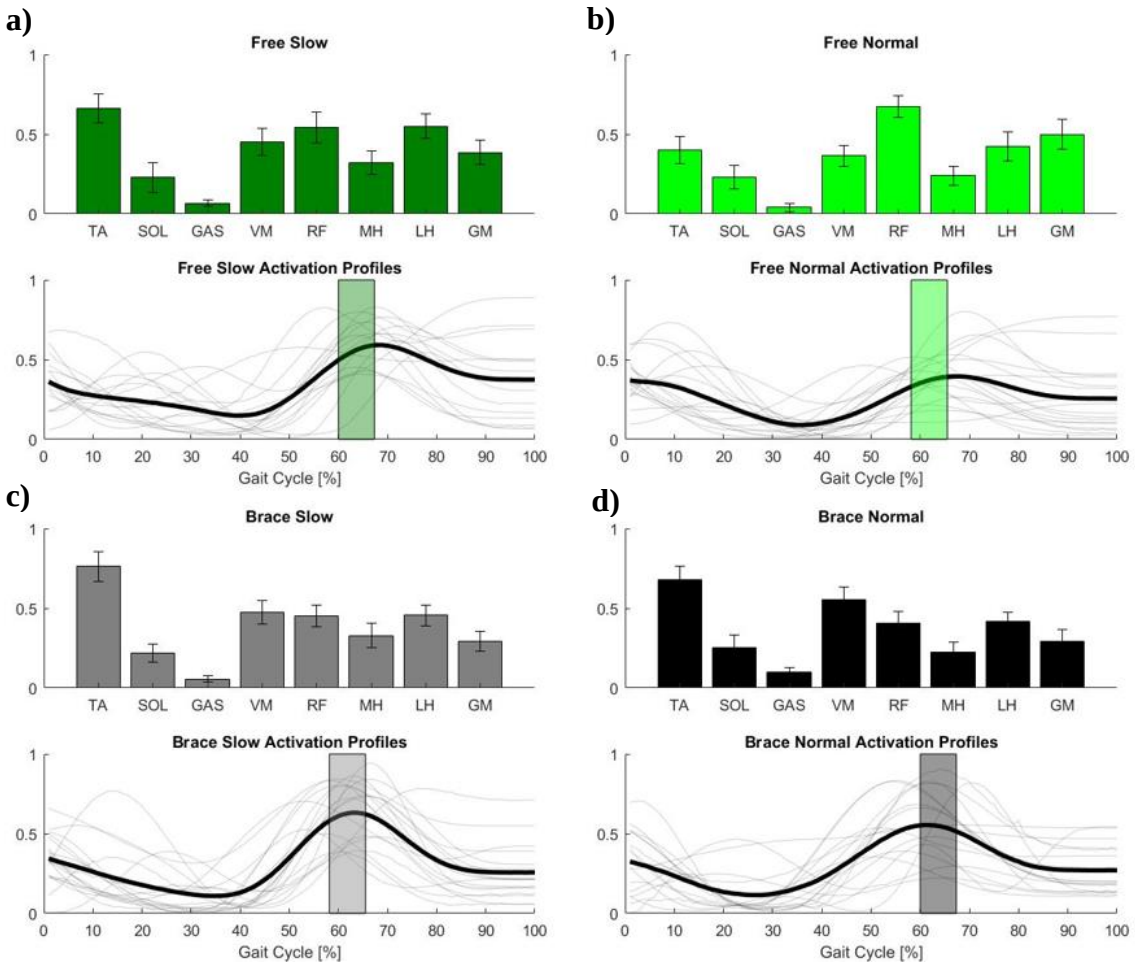

Figure 4: Each quadrant represents the corresponding pre-swing (shaded region) module for the two conditions, *Free* and *Brace,* at slow and normal walking speeds and shows the weight contribution of each muscle for that module (top) and the activation of the module throughout a gait cycle (bottom).

Table 2: Corresponding Spearman correlation values for comparing similarity in module compositions within the healthy conditions

	Free Slow-Free Normal	Free Slow-Brace Normal	Brace Slow-Free Slow	Brace Slow-Free Normal	Brace Slow-Brace Normal	Brace Normal-Free Normal
Module Correlation	0.714	0.905	0.905	0.476	0.929	0.548

IEMG ANALYSIS

There was a main effect of knee restriction for the iEMG analysis, the TA (t = 4.084, $p < 0.001$) and VM (t = 2.045, $p < 0.05$) both showed higher activity as a result of the knee restriction. Between the *Brace* and *Free* conditions, there was a difference in the MH (t = 2.139, $p < 0.05$) showing higher iEMG activity in the *Free* for the slow conditions. The GAS showed a strong trend (t = 1.958, p = 0.06) of being higher in the *Brace* than the *Free*.

For the normal walking condition, the TA showed (t = 4.212, $p < 0.001$) greater activity as well as the VM (t = 2.429, $p < 0.05$) in *Brace* than in *Free.*

Walking speed also played a key role in the amount of iEMG generated to progress through the gait motion. The TA (t = 2.001, p = 0.052) showed a strong trend of being higher as the walking speed was reduced meanwhile the SOL (t = 1.86, $p < 0.07$) , GAS (t = 4.309, $p < 0.001$), VM (t = 2.534, $p < 0.05$) and GM (t = 2.144, $p < 0.05$) all showed higher iEMG magnitudes at the normal walking speed. At the greater walking speed for the *Brace* conditions, GAS (t = 3.308, $p < 0.01$) and VM (t = 2.649, $p < 0.05$) both showed higher activity. For the *Free* condition, the normal walking speed resulted in higher GAS (t = 3.141, $p < 0.01$) and RF (t = 2.035, $p < 0.05$) while slower walking speed showed greater TA (t = 3.541, $p < 0.01$) and MH (t = 3.372, $p < 0.01$). Results are summarized in Figure 5.

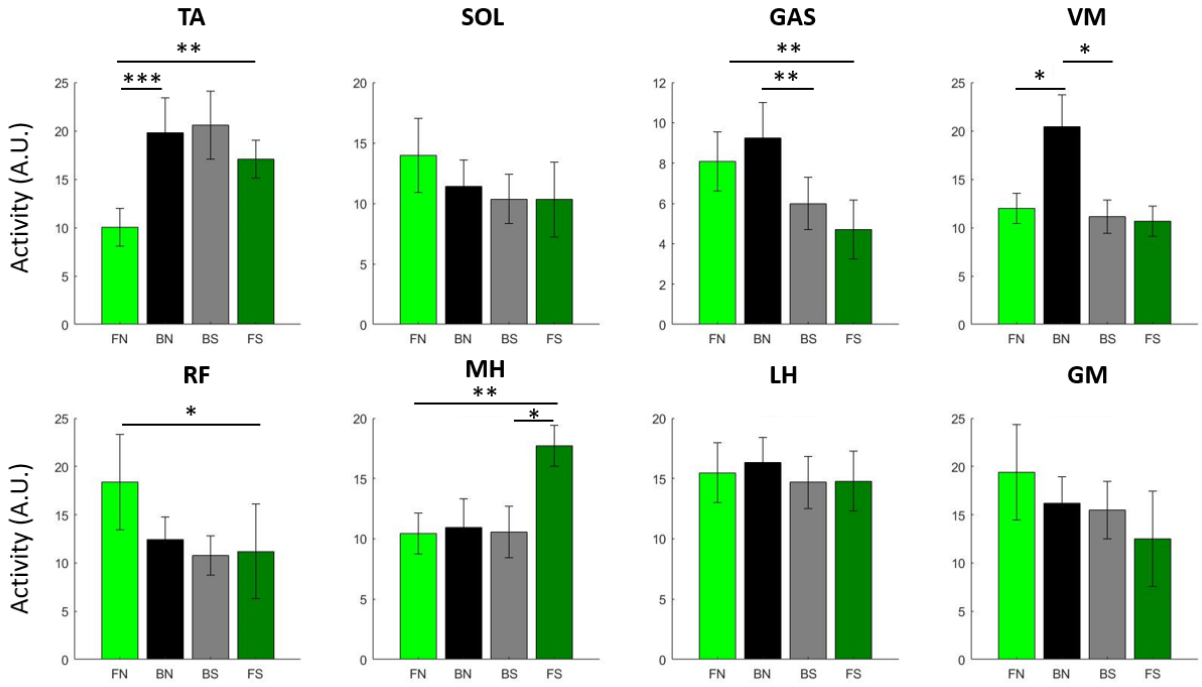

Figure 5: iEMG results for all eight muscles within the healthy conditions. Where FS and BS refer to *Free* and *Brace* for the slow walking condition and FN and BN refer to *Free* and *Brace* for the normal walking condition. The level of significance between the conditions are denoted as * $p < 0.05$, ** $p < 0.01$, *** $p < 0.001$.

COMPARISONS TO POST-STROKE POPULATION

KINEMATIC AND SPATIOTEMPORAL COMPARISONS

The ages between the healthy (45±11) and *SKG* (58±11) were found to be significant ($p < 0.01$) as were the ages between the healthy (45±11) and *NSKG* (55±15) ($p < 0.05$). However, the gait speeds between the groups were found to be similar between both *Brace* and *SKG* ($p = 0.26$) as well as *Brace* and *NSKG* ($p = 0.77$). Comparison of kinematic measures between the healthy and post-stroke groups were conducted to view any differences between those mechanically restricted as opposed to those with a neural

impairment (Figure 6). We found similar kinematics for the two post-stroke groups despite the lack of knee flexion ROM ($t = 5.654$, $p < 0.001$) being the only significant kinematic variable between the two groups (Table 3). In order to provide an accurate comparison of the two groups, healthy and stroke, we used the slower walking speeds from our experiment and observed the kinematic differences. We found higher knee ROM ($t = 12.57$, $p < 0.001$), ankle ROM ($t = 2.678$, $p < 0.05$), but less hip abduction ROM ($t = 2.157$, $p < 0.05$) for the *Free* condition when compared to the *SKG* group. No significant differences were found between the *Brace* condition and the *SKG* group for the kinematic variables. Comparing the *Free* to the *NSKG* group, we saw greater hip abduction ROM ($t = 4.321$, $p < 0.001$) and lower values for the knee ROM ($t = 2.059$, $p < 0.05$) and ankle ROM ($t = 2.491$, $p < 0.05$ for the *NSKG* group. The hip ($t = 3.16$, $p < 0.01$) and knee ROM ($t = 5.277$, $p < 0.001$) were both lower for the *Brace* when compared to *NSKG* but greater stance ratio ($t = 2.059$, $p < 0.05$) was shown by *Brace.*

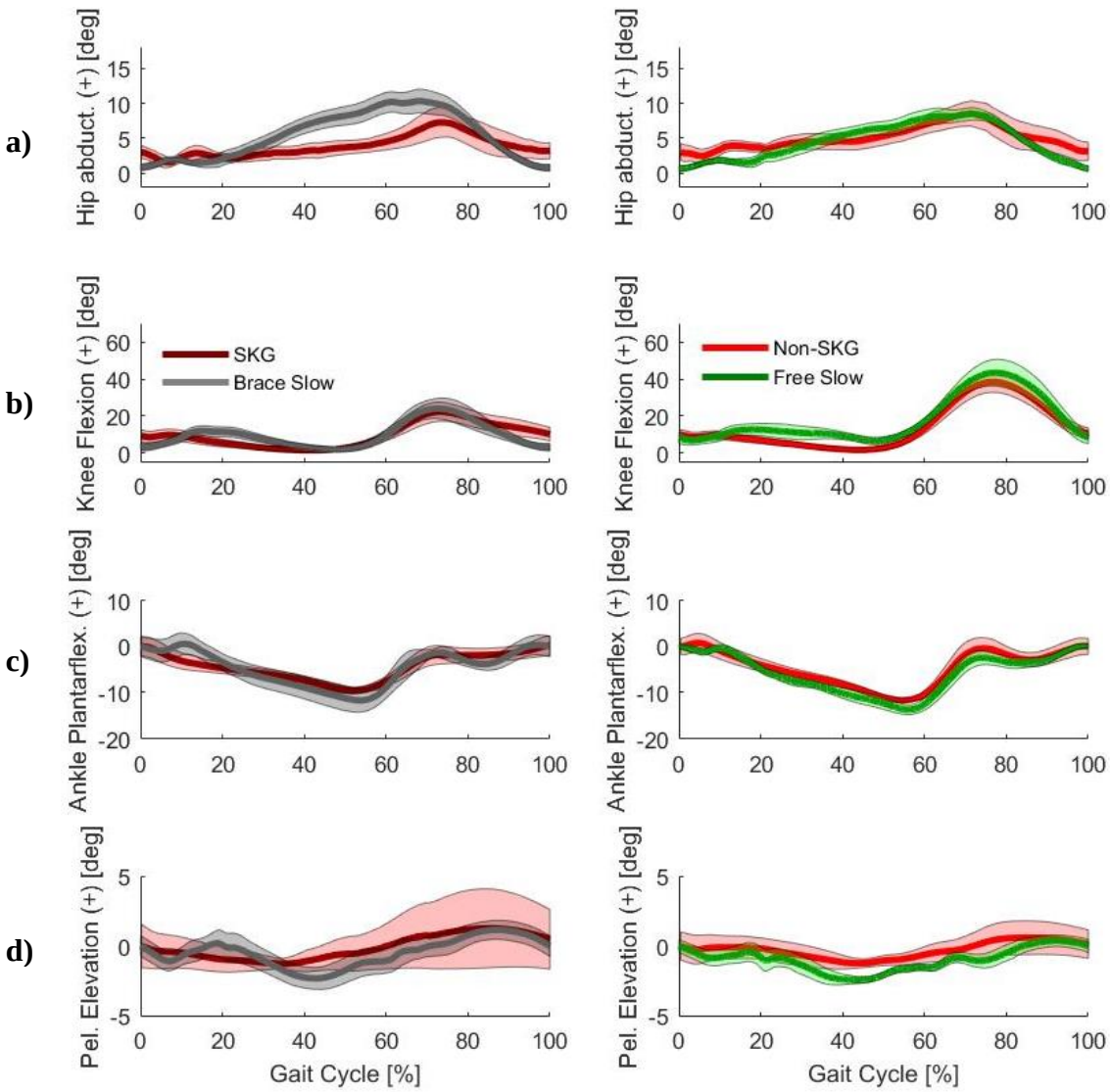

Figure 6: The hip abduction (a), knee flexion (b), ankle plantarflexion (c) and pelvic obliquity (d) angles for the constrained side under different conditions (*Brace* and *Free*) are given for slow speed which are compared to their post-stroke counterparts.

Table 3: Summary of the joint angle ROM and spatiotemporal gait measures for healthy and post-stroke gait. The measures display the mean values and standard deviations. The level of significance between *Free* and *NSKG* are denoted as # $p < 0.05$, ## $p < 0.01$, ### $p < 0.001$; between *Free* and *SKG* denoted as ŧ $p < 0.05$, ŧŧ $p < 0.01$, ŧŧŧ $p < 0.001$; between the *Brace* and *NSKG* conditions denoted as: ‡ $p < 0.05$, ‡‡ $p < 0.01$, ‡‡‡ $p < 0.001$; between the *Brace* and *SKG* conditions denoted as * $p < 0.05$, ** $p < 0.01$, *** $p < 0.001$; between the two stroke conditions *SKG* and *NSKG* denoted as ¥ $p < 0.05$, ¥¥ $p < 0.01$, ¥¥¥ $p < 0.001$.

Outcome Measures \ Group		**Free Slow**	**Brace Slow**	**SKG**	**NSKG**
Kinematic Measures	Knee ROM (°)	$51.5 \pm 9.85^{\#, ŧŧŧ}$	$23.0 \pm 12.4^{‡‡‡}$	$25.4 \pm 8.64^{¥¥¥}$	43.1 ± 13.9
	Hip abd. ROM (°)	$10.8 \pm 2.86^{\#\#\#, ŧ}$	$11.6 \pm 4.12^{‡‡}$	13.2 ± 3.39	15.1 ± 3.45
	Ankle ROM (°)	$23.7 \pm 12.2^{\#, ŧ}$	18.3 ± 10.5	16.1 ± 2.85	17.7 ± 3.96
	Pel obl. ROM (°)	3.70 ± 1.46	4.78 ± 1.22	7.11 ± 4.34	4.96 ± 1.81
Spatiotemporal	Stance Ratio	$0.98 \pm 0.02^{\#\#\#,ŧŧŧ}$	$0.95 \pm 0.04^{‡, *}$	0.92 ± 0.03	0.92 ± 0.04
	Cadence	$107 \pm 9.78^{\#\#\#, ŧŧŧ}$	93.0 ± 6.72	84.2 ± 22.0	87.6 ± 11.5
	Step Length	$0.36 \pm 0.07^{‡‡‡, ŧŧŧ}$	$0.38 \pm 0.09^{***}$	$0.22 \pm 0.10^{¥}$	0.31 ± 0.15

QUANTITATIVE MODULE ANALYSIS

The *Free* (3.7) and *Brace* (3.5) condition exhibited a similar number of modules to the *SKG* (3.1) and *NSKG* (3.4) subjects (Figure 7).

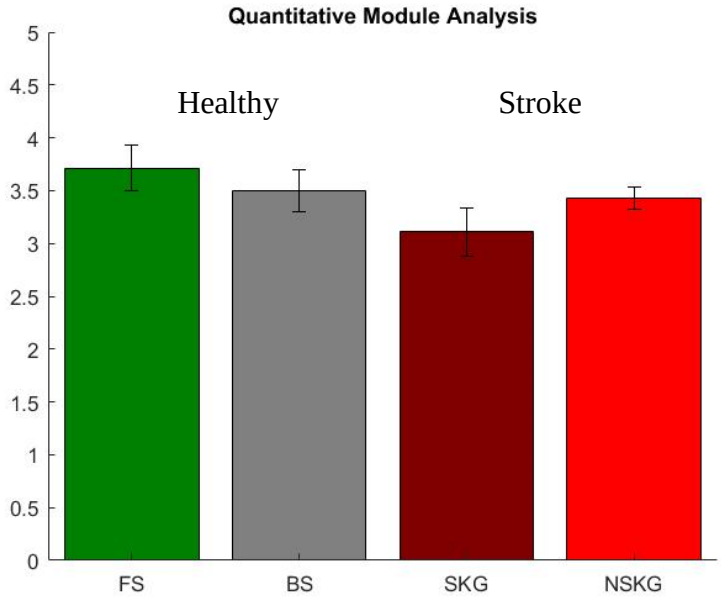

Figure 7: Number of modules exhibited between the slow healthy conditions and the two stroke groups. No significant differences were found between the groups

MODULE COMPOSITION

Comparing the two stroke conditions, there is similar TA contributions in both but a greater use of the GAS in the *SKG* while the *NSKG* shows more contribution from the MH as the group is able to attain a greater range of motion with their knee joint (Figure 8). Table 4 shows similarity of modules between the healthy and stroke groups. The coordination pattern for the two stroke groups were fairly dissimilar despite coming from the same population (Spearman's $\rho = 0.524$). The *Free* and *NSKG* exhibited the highest correlation between healthy and stroke groups (Spearman's $\rho = 0.833$). As expected, the

Free condition module was not similar (Spearman's $\rho = 0.167$) at all when compared to *SKG*. Despite the greater knee ROM exhibited by the *NSKG* group, the corresponding pre-swing module was much more similar to the *Brace* condition (Spearman's $\rho = 0.643$) than the *SKG* group which resulted in vastly dissimilar patterns despite similar kinematics (Spearman's $\rho = -0.024$). Lastly, looking at the co-contraction measure, we found the *Free* (1.14), *Brace* (1.18) and *NSKG* (1.19) all showed similar relative contributions while the *SKG* (1.42) showed greater contributions from the quadriceps.

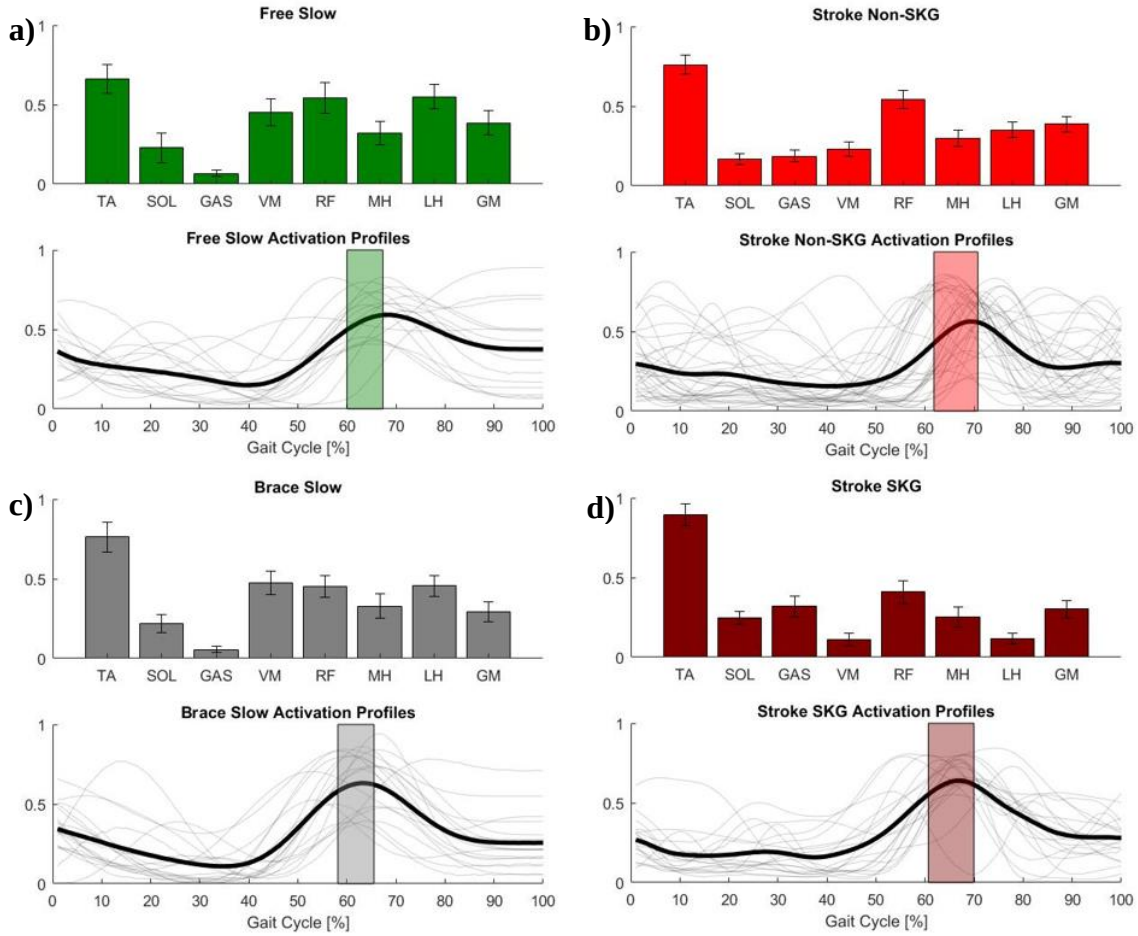

Figure 8: Each quadrant represents the corresponding pre-swing module (shaded region) for the two conditions, *Free* and *Brace*, at slow walking speeds and the two extracted stroke groups, *SKG* and *NSKG*, shows the weight contribution of each muscle for that module (top) and the activation of the module throughout a gait cycle (bottom).

Table 4: Corresponding Spearman correlation values for comparing similarity in module compositions between the healthy and stroke groups

	Brace Slow-SKG	**Brace Slow-NSKG**	**Free Slow-SKG**	**Free Slow-NSKG**	**SKG-NSKG**
Module Correlation	-0.024	0.643	0.167	0.833	0.524

Chapter 4: Discussion

Our previous work showed that hip abduction is not a compensatory mechanism for reduced knee flexion angle (Akbas et al., 2019a, 2019b; Sulzer et al., 2010) suggesting that neurally based gait deviations may play a larger role than previously realized. Our goal was to determine the muscle coordination adaptation to mechanical knee restriction and compare the results to those with both restricted knee flexion and neural impairment. We applied kinematic constraints at the knee in healthy individuals to imitate the sagittal plane kinematics of post-stroke SKG and assessed the resulting coordination patterns using NNMF and iEMG. We found that mechanically restricting healthy individuals at the knee did not substantially influence the gait coordination pattern during the pre-swing phase. However, we found that the greatest difference in coordination patterns was observed between those with post-stroke SKG and healthy individuals with reduced knee flexion, providing the template to separate the mechanical from neural adaptations to post-stroke SKG.

The kinematic results for ROM throughout the pre-swing and swing phase coincide with our previous finding where healthy individuals with restricted kinematics exhibited lesser hip abduction than post-stroke individuals (Akbas et al., 2019b). We were able to replicate the kinematics from our previous study showing reduced knee flexion similar to post-stroke SKG individuals (Akbas et al., 2019b). Additionally, we saw no changes in hip abduction as a result of the brace but greater ROM from the *SKG* population which aligned with our previous findings (Akbas et al., 2019b).

The mechanical knee restriction elicited compensatory strategies. The spatiotemporal characteristics found a reduced stance ratio for both restricted conditions indicating a quicker stride on the restricted limb as the amount of push-off is reduced due

to the reduction in ankle plantarflexion. Both analyses, NNMF and iEMG, show largely similar muscle coordination patterns between conditions, with the most likely compensatory muscle being the TA. This follows the kinematic behavior we observed in our previous work where greater dorsiflexion was found in the pre-swing phase to attain toe clearance (Akbas et al., 2019b). The iEMG also found the GAS activity increased as a result of gait speed indicating the importance of plantar flexor contributions to body support and swing initiation (Neptune et al., 2001; Zajac et al., 2003). However, despite the greater MH activity in slow walking *Free* condition, the similarity of LH activity for all four conditions was the main finding from the iEMG analysis. While post-stroke individuals lack of knee flexion is attributed to hamstrings weakness (Neckel et al., 2006), we observed similar LH activity perhaps suggesting active recruitment of hamstrings from healthy individuals despite a kinematic restriction. Additionally, given the similarity between the pre-swing modules for *Free* and *Brace* at the slow speed, the modules closely represent the flexion/ground clearance module reported in Clark et al. (2010). Thus, while we observed muscular compensations in response to the reduced knee flexion, the gait patterns between *Brace* and *Free* conditions resulted in similar composition to each other and prior literature.

Despite similar gait function (in terms of gait speed) and number of motor modules, the *SKG* and *NSKG* groups were only moderately similar in pre-swing muscle coordination. The relative contribution of majority of the muscles appear to show a reduction throughout the pre-swing phase indicating either dominance of certain muscles (i.e. RF to stiffen the leg), muscle weakness or self-regulation of muscle recruitment (lack of hamstrings activity) (Neckel et al., 2006). The module compositions also follow similar trends to that reported in literature where the two primary contributors to this phase are the TA and RF

(Clark et al., 2010). However, it is difficult to decipher the levels of muscle activity contribution due to reduced knee flexion because of the grouping of all post-stroke individuals into one population. The reduced similarity in muscle coordination patterns between these two groups could be due to different walking kinematics, abnormal timing of hamstrings activation or altered neural conditions (Den Otter et al., 2007; Kerrigan et al., 1991).

We isolated the contribution of neural impairments to altered muscle coordination by simulating the characteristic mechanical impairment in *SKG* on healthy individuals, comparing the results to those with *SKG* at a similar speed. In parallel, we compared speed-matched walking without knee restriction to those post-stroke without SKG. Comparing pre-swing muscle coordination patterns of the latter pair shows similar module compositions (Spearman's $\rho = 0.833$), *SKG* was very different than the group's healthy counterpart (Spearman's $\rho = -0.024$). Despite both respective groups exhibiting similar kinematics, the disparity in correlation values suggest the *SKG* group may have greater abnormal coordination than the *NSKG*. The primary similarity between all of the modules was the large usage of TA which not only assists in providing toe clearance but also acts to accelerate the knee into flexion (Neptune et al., 2009). The main contributing muscles to these differences in the *SKG* group was a reduction in VM and LH and an increase in GAS. While we initially expected GM to contribute to this difference, the sampled SKG group did not show exaggerated hip abduction, so the result is not surprising. The reduced relative VM activity could be reflecting the dominance of the RF in both groups, which appears to be the primary contributor to *SKG* in post-stroke populations (Chantraine et al., 2005; Tenniglo et al., 2014). It has also been reported that weakness of muscles following stroke could be due to co-contraction of antagonistic muscles (Chae and Yu, 2002;

Knutsson and Mårtensson, 1980; Knutsson and Richards, 1979). Therefore, looking at the ratio of relative weightings of the quadriceps over the hamstrings, we see greater relative quadriceps contribution in the *SKG* group compared to other groups which could be a contributing factor to both hamstring weakness and lack of knee flexion exhibited (Neckel et al., 2006). This finding aligns with previous research indicating overactivity of the quadriceps, specifically the RF, being a primary contributor to impairment during gait for post-stroke SKG individuals (Chantraine et al., 2005; Goldberg et al., 2004; Kerrigan et al., 2000; Reinbolt et al., 2008; Stoquart et al., 2008; Waters et al., 1979).

LIMITATIONS AND FUTURE WORK

There are limitations to the study which prevent greater generalizations. We were not able to recruit age-matched subjects for this experiment, however, there are studies which show motor modules are not dependent on age (Artoni et al., 2013; Monaco et al., 2010). Factors such as cadence and biomechanical demand which are governed by gait speed, which was found to be similar between the groups, are primary contributors to number of modules. Our comparisons did not simulate motor control or proprioceptive contributions to gait compensations. While it is possible proprioceptive loss could be a factor for increased hip abduction in post-stroke SKG, it is unlikely this would result in a compensation with great energetic cost. As previously mentioned, the number of modules are dependent on the gait speed at which the data is recorded. The stroke population was able to self-select their walking speed while healthy individuals in our experiment were tasked with walking at two set speeds, 0.5 m/s and 1 m/s. However, the two walking speeds chosen for this experiment represent similar walking speeds to the post-stroke group and typical comfortable healthy walking speeds and therefore are still representative speeds for both populations. Additionally, to account for other modules active during the pre-swing

phase, the multi-factorial method to determine active modules assisted in extracting all possible muscle activity. Kinematic and muscle activity factors were looked at for adaptation to the brace and a decrease in muscle activity was observed. We accounted for adaptation to the brace by observing the final one-third of the data collection, however, individuals in the post-stroke population had a mean time since stroke of 42 months, therefore, the two-minute simulation of post-stroke kinematics may not be a substantial amount of time for an accurate comparison.

For this study, we were primarily focused on the pre-swing phase of the gait cycle, however, further analysis of the modules may reveal more to the story regarding post-stroke abnormal coordination throughout the entire gait phase. Other methods which may provide greater insight into the emergence of radically different coordination patterns include instructing healthy individuals with restricted knee kinematics to match hip circumduction such that the gait pattern better mimics what is observed in post-stroke SKG. Since the brace provides an accurate model to imitate post-stroke SKG kinematics, applying the kinematic constraint to activities of daily living such as climbing, stepping down and turning in hopes of extrapolating abnormal muscle coordination patterns which may assist in reducing the risk of falling for the given tasks.

Chapter 5: Conclusions

We implemented a novel technique to imitate post-stroke SKG kinematics in healthy individuals, performed coordination analysis and compared the resulting patterns to a cohort of post-stroke individuals. Despite the addition of a mechanical restriction to knee flexion, modular recruitment of muscles did not vary the coordination patterns greatly in healthy individuals suggesting regulated activity of muscles. Our data shows different coordination patterns being recruited between the groups suggesting kinematic constraints are not enough to account for the copious amount of impairments which result from a stroke suggesting the role of abnormal coordination. We found that TA compensates as a result of reduced knee flexion in efforts to clear the toe despite its secondary purpose to accelerate the knee into swing for both healthy and impaired populations, but lack of VM activity in both stroke groups possibly stems from abnormal coordination (Neptune et al., 2009). It is likely that overactivity of the knee extensors, primarily RF, in conjunction with spasticity and abnormal stretch reflex coupling during the pre-swing phase culminate to create an abnormal movement pattern of the paretic limb (Akbas et al., 2019a). The work we have done provides a gateway to potentially delineating potential factors of abnormal coordination and motivation for interventions, robotic or traditional, to develop more accurate treatment strategies and regimens.

Appendix

Table A1: Demographics of healthy participants

Subject no	Age (yrs)	G	W (kg.)	H (m)	Dominant Side
1	53	F	55.8	1.66	R
2	45	M	56.7	1.72	R
3	49	F	54.4	1.35	R
4	30	M	90.3	1.92	R
5	39	M	72.6	1.70	R
6	69	M	83.9	1.80	R
7	54	M	75.3	1.63	R
8	49	M	72.6	1.73	R
9	51	M	93.0	1.78	L
10	33	M	74.8	1.82	R
11	49	F	72.6	1.78	R
12	334	M	72.6	1.68	R
13	52	F	64.4	1.52	R
14	29	M	74.8	1.73	R
Mean	45.4 ± 11.2		72.4 ± 11.8	1.70 ± 0.14	

Table A2: Demographics of post-stroke stiff knee gait participants

Subject no	Age (yrs)	G	W (kg.)	Speed (m/s)	Dominant Side	Time Since Stroke
1	43	M	84.9	0.20	L	6
3	40	M	96.2	0.10	R	6
4	66	M	98.5	0.40	R	127
5	50	M	115.7	0.25	R	24
8	48	M	114.7	0.75	R	20
9	58	M	115.3	0.15	L	6
10	70	M	86.4	0.30	R	29
12	63	M	114.6	0.40	R	54
13	61	M	92.5	0.15	L	6
15	70	M	85	0.30	R	47
16	75	M	66.6	0.44	R	49
21	59	M	74.3	0.30	L	11
33	62	M	84.9	0.25	R	82
35	82	M	70.9	0.30	L	3
41	49	M	94.3	0.45	R	11
42	55	F	53.7	0.30	L	81
43	60	M	75.8	0.45	R	26
46	49	M	113.8	0.15	L	6
Mean	58.9 ± 11.2		91.0 ± 18.7	0.31 ± 0.15		33 ± 34

Table A3: Demographics of post-stroke non-stiff knee gait participants

Subject no	Age (yrs)	G	W (kg.)	Speed (m/s)	Dominant Side	Time Since Stroke (mo.)
2	71	F	70.3	0.10	R	6
6	58	F	74.1	0.10	R	34
7	25	F	78.5	0.15	L	20
11	69	F	74.1	0.20	L	6
14	70	F	103.8	0.15	R	6
17	72	M	138.2	0.70	R	6
18	67	F	76.1	0.55	R	20
19	56	F	88.1	0.55	R	137
20	58	F	76.8	0.55	R	9
22	60	M	107	0.60	R	63
23	68	M	94.1	0.75	R	8
24	71	F	101.9	0.15	L	6
25	51	M	85.9	0.55	L	6
26	28	F	78.6	0.55	L	40
27	68	M	120.1	0.55	L	25
28	53	F	112.7	0.35	L	28
29	42	F	87.6	0.80	R	33
30	62	M	87.8	0.65	R	99
31	50	M	134.3	0.50	R	67
32	58	M	105.9	0.65	R	8
34	26	F	77.7	0.30	L	33
36	49	M	93.5	0.40	R	19
37	35	F	63.7	0.50	R	21
38	76	F	91.5	0.45	R	7
39	59	M	110.9	0.70	R	11
40	33	M	68.7	0.20	L	134
44	64	F	107.2	0.30	L	24
45	41	M	74.9	0.20	L	8
Mean	55.0 ± 15.1		92.3 ± 19.5	0.44 ± 0.22		31.6 ± 36.6

References

Akbas, T., Neptune, R.R., Sulzer, J., 2019a. Neuromusculoskeletal Simulation Reveals Abnormal Rectus Femoris-Gluteus Medius Coupling in Post-stroke Gait. Front. Neurol. 10. https://doi.org/10.3389/fneur.2019.00301

Akbas, T., Prajapati, S., Ziemnicki, D., Tamma, P., Gross, S., Sulzer, J., 2019b. Hip circumduction is not a compensation for reduced knee flexion angle during gait. Journal of Biomechanics 87, 150–156. https://doi.org/10.1016/j.jbiomech.2019.02.026

Artoni, F., Monaco, V., Micera, S., 2013. Selecting the best number of synergies in gait: Preliminary results on young and elderly people, in: 2013 IEEE 13th International Conference on Rehabilitation Robotics (ICORR). Presented at the 2013 IEEE 13th International Conference on Rehabilitation Robotics (ICORR), pp. 1–5. https://doi.org/10.1109/ICORR.2013.6650416

Barroso, F.O., Torricelli, D., Molina-Rueda, F., Alguacil-Diego, I.M., Cano-de-la-Cuerda, R., Santos, C., Moreno, J.C., Miangolarra-Page, J.C., Pons, J.L., 2017. Combining muscle synergies and biomechanical analysis to assess gait in stroke patients. Journal of Biomechanics 63, 98–103. https://doi.org/10.1016/j.jbiomech.2017.08.006

Benjamin Emelia J., Virani Salim S., Callaway Clifton W., Chamberlain Alanna M., Chang Alexander R., Cheng Susan, Chiuve Stephanie E., Cushman Mary, Delling Francesca N., Deo Rajat, de Ferranti Sarah D., Ferguson Jane F., Fornage Myriam, Gillespie Cathleen, Isasi Carmen R., Jiménez Monik C., Jordan Lori Chaffin, Judd Suzanne E., Lackland Daniel, Lichtman Judith H., Lisabeth Lynda, Liu Simin, Longenecker Chris T., Lutsey Pamela L., Mackey Jason S., Matchar David B., Matsushita Kunihiro, Mussolino Michael E., Nasir Khurram, O'Flaherty Martin, Palaniappan Latha P., Pandey Ambarish, Pandey Dilip K., Reeves Mathew J., Ritchey Matthew D., Rodriguez Carlos J., Roth Gregory A., Rosamond Wayne D., Sampson Uchechukwu K.A., Satou Gary M., Shah Svati H., Spartano Nicole L., Tirschwell David L., Tsao Connie W., Voeks Jenifer H., Willey Joshua Z., Wilkins John T., Wu Jason HY., Alger Heather M., Wong Sally S., Muntner Paul, 2018. Heart Disease and Stroke Statistics—2018 Update: A Report From the American Heart Association. Circulation 137, e67–e492. https://doi.org/10.1161/CIR.0000000000000558

Bobath, B., 1999. Adult hemiplegia: evaluation and treatment. Butterworth-Heinemann., Oxford.

Brough, L.G., Kautz, S.A., Bowden, M.G., Gregory, C.M., Neptune, R.R., 2019. Merged plantarflexor muscle activity is predictive of poor walking performance in post-stroke hemiparetic subjects. Journal of Biomechanics 82, 361–367. https://doi.org/10.1016/j.jbiomech.2018.11.011

Campanini, I., Merlo, A., Damiano, B., 2013. A method to differentiate the causes of stiff-knee gait in stroke patients. Gait & Posture 38, 165–169. https://doi.org/10.1016/j.gaitpost.2013.05.003

Chae, J., Yu, D.T., 2002. Neuromuscular Electrical Stimulation for Motor Restoration in Hemiparesis. Topics in Stroke Rehabilitation 8, 24–39. https://doi.org/10.1310/REXB-AKV9-2XBE-U5QA

Chantraine, F., Detrembleur, C., Lejeune, T., 2005. Effect of the rectus femoris motor branch block on post-stroke stiff-legged gait. Acta neurologica Belgica 105, 171–177.

Clark, D.J., Ting, L.H., Zajac, F.E., Neptune, R.R., Kautz, S.A., 2009. Merging of Healthy Motor Modules Predicts Reduced Locomotor Performance and Muscle Coordination Complexity Post-Stroke. Journal of Neurophysiology 103, 844–857. https://doi.org/10.1152/jn.00825.2009

Cruz, T.H., Dhaher, Y.Y., 2008. Evidence of Abnormal Lower-Limb Torque Coupling After Stroke. Stroke 39, 139–147. https://doi.org/10.1161/STROKEAHA.107.492413

Cruz, T.H., Lewek, M.D., Dhaher, Y.Y., 2009. Biomechanical impairments and gait adaptations post-stroke: Multi-factorial associations. Journal of Biomechanics 42, 1673–1677. https://doi.org/10.1016/j.jbiomech.2009.04.015

Den Otter, A.R., Geurts, A.C.H., Mulder, Th., Duysens, J., 2007. Abnormalities in the temporal patterning of lower extremity muscle activity in hemiparetic gait. Gait & Posture 25, 342–352. https://doi.org/10.1016/j.gaitpost.2006.04.007

Finley, J.M., Perreault, E.J., Dhaher, Y.Y., 2008. Stretch reflex coupling between the hip and knee: implications for impaired gait following stroke. Exp Brain Res 188, 529. https://doi.org/10.1007/s00221-008-1383-z

Goldberg, S.R., Anderson, F.C., Pandy, M.G., Delp, S.L., 2004. Muscles that influence knee flexion velocity in double support: implications for stiff-knee gait. Journal of Biomechanics 37, 1189–1196. https://doi.org/10.1016/j.jbiomech.2003.12.005

Goldberg, S.R., Õunpuu, S., Arnold, A.S., Gage, J.R., Delp, S.L., 2006. Kinematic and kinetic factors that correlate with improved knee flexion following treatment for stiff-knee gait. Journal of Biomechanics 39, 689–698. https://doi.org/10.1016/j.jbiomech.2005.01.015

Kerrigan, D.C., Frates, E.P., Rogan, S., Riley, P.O., 2000. Hip hiking and circumduction: quantitative definitions. Am J Phys Med Rehabil 79, 247–252.

Kerrigan, D.C., Gronley, J., Perry, J., 1991. Stiff-legged gait in spastic paresis. A study of quadriceps and hamstrings muscle activity. Am J Phys Med Rehabil 70, 294–300.

Knutsson, E., Mårtensson, A., 1980. Dynamic motor capacity in spastic paresis and its relation to prime mover dysfunction, spastic reflexes and antagonist co-activation. Scand J Rehabil Med 12, 93–106.

Knutsson, E., Richards, C., 1979. Different types of disturbed motor control in gait of hemiparetic patients. Brain 102, 405–430. https://doi.org/10.1093/brain/102.2.405

Lee, D.D., Seung, H.S., 1999. Learning the parts of objects by non-negative matrix factorization. Nature 401, 788. https://doi.org/10.1038/44565

Lelas, J.L., Merriman, G.J., Riley, P.O., Kerrigan, D.C., 2003. Predicting peak kinematic and kinetic parameters from gait speed. Gait & Posture 17, 106–112. https://doi.org/10.1016/S0966-6362(02)00060-7

Lewek, M.D., Osborn, A.J., Wutzke, C.J., 2012. The Influence of Mechanically and Physiologically Imposed Stiff-Knee Gait Patterns on the Energy Cost of Walking. Archives of Physical Medicine and Rehabilitation 93, 123–128. https://doi.org/10.1016/j.apmr.2011.08.019

Michaud, S.D., Gard, S.A., Childress, D.S., 2000. A preliminary investigation of pelvic obliquity patterns during gait in persons with transtibial and transfemoral amputation. Journal of rehabilitation research and development 37, 1–10.

Monaco, V., Ghionzoli, A., Micera, S., 2010. Age-Related Modifications of Muscle Synergies and Spinal Cord Activity During Locomotion. Journal of Neurophysiology 104, 2092–2102. https://doi.org/10.1152/jn.00525.2009

Neckel, N., Pelliccio, M., Nichols, D., Hidler, J., 2006. Quantification of functional weakness and abnormal synergy patterns in the lower limb of individuals with chronic stroke. Journal of NeuroEngineering and Rehabilitation 3, 17. https://doi.org/10.1186/1743-0003-3-17

Neptune, R.R., Clark, D.J., Kautz, S.A., 2009. Modular control of human walking: A simulation study. Journal of Biomechanics 42, 1282–1287. https://doi.org/10.1016/j.jbiomech.2009.03.009

Neptune, R.R., Kautz, S.A., Zajac, F.E., 2001. Contributions of the individual ankle plantar flexors to support, forward progression and swing initiation during walking. Journal of Biomechanics 34, 1387–1398. https://doi.org/10.1016/S0021-9290(01)00105-1

Perry, J., K, S.T., Davids, J.R., 1992. Gait Analysis: Normal and Pathological Function. Journal of Pediatric Orthopaedics 12, 815.

Reinbolt, J.A., Fox, M.D., Arnold, A.S., Õunpuu, S., Delp, S.L., 2008. Importance of preswing rectus femoris activity in stiff-knee gait. Journal of Biomechanics 41, 2362–2369. https://doi.org/10.1016/j.jbiomech.2008.05.030

Routson, R.L., Clark, D.J., Bowden, M.G., Kautz, S.A., Neptune, R.R., 2013. The influence of locomotor rehabilitation on module quality and post-stroke hemiparetic walking performance. Gait & Posture 38, 511–517. https://doi.org/10.1016/j.gaitpost.2013.01.020

Safavynia, S., Torres-Oviedo, G., Ting, L., 2011. Muscle Synergies: Implications for Clinical Evaluation and Rehabilitation of Movement. Topics in Spinal Cord Injury Rehabilitation 17, 16–24. https://doi.org/10.1310/sci1701-16

Stoquart, G.G., Detrembleur, C., Palumbo, S., Deltombe, T., Lejeune, T.M., 2008. Effect of Botulinum Toxin Injection in the Rectus Femoris on Stiff-Knee Gait in People With Stroke: A Prospective Observational Study. Archives of Physical Medicine and Rehabilitation 89, 56–61. https://doi.org/10.1016/j.apmr.2007.08.131

Sulzer James S., Gordon Keith E., Dhaher Yasin Y., Peshkin Michael A., Patton James L., 2010. Preswing Knee Flexion Assistance Is Coupled With Hip Abduction in People With Stiff-Knee Gait After Stroke. Stroke 41, 1709–1714. https://doi.org/10.1161/STROKEAHA.110.586917

Tenniglo, M.J., Nederhand, M.J., Prinsen, E.C., Nene, A.V., Rietman, J.S., Buurke, J.H., 2014. Effect of Chemodenervation of the Rectus Femoris Muscle in Adults With a Stiff Knee Gait Due to Spastic Paresis: A Systematic Review With a Meta-Analysis in Patients With Stroke. Archives of Physical Medicine and Rehabilitation 95, 576–587. https://doi.org/10.1016/j.apmr.2013.11.008

Thawrani, D., Haumont, T., Church, C., Holmes, L., Dabney, K.W., Miller, F., 2012. Rectus Femoris Transfer Improves Stiff Knee Gait in Children With Spastic Cerebral Palsy. Clin Orthop Relat Res 470, 1303–1311. https://doi.org/10.1007/s11999-011-2215-1

Ting, L.H., Macpherson, J.M., 2005. A Limited Set of Muscle Synergies for Force Control During a Postural Task. Journal of Neurophysiology 93, 609–613. https://doi.org/10.1152/jn.00681.2004

Vance, J., Wulf, G., Töllner, T., McNevin, N., Mercer, J., 2004. EMG Activity as a Function of the Performer's Focus of Attention. Journal of Motor Behavior 36, 450–459. https://doi.org/10.3200/JMBR.36.4.450-459

Waters, R.L., Garland, D.E., Perry, J., Habig, T., Slabaugh, P., 1979. Stiff-legged gait in hemiplegia: surgical correction. J Bone Joint Surg Am 61, 927–933.

Watkins, C.L., Leathley, M.J., Gregson, J.M., Moore, A.P., Smith, T.L., Sharma, A.K., 2002. Prevalence of spasticity post stroke. Clin Rehabil 16, 515–522. https://doi.org/10.1191/0269215502cr512oa

Yokoyama, H., Ogawa, T., Kawashima, N., Shinya, M., Nakazawa, K., 2016. Distinct sets of locomotor modules control the speed and modes of human locomotion. Scientific Reports 6, 36275. https://doi.org/10.1038/srep36275

Zajac, F.E., Neptune, R.R., Kautz, S.A., 2003. Biomechanics and muscle coordination of human walking: Part II: Lessons from dynamical simulations and clinical implications. Gait & Posture 17, 1–17. https://doi.org/10.1016/S0966-6362(02)00069-3

Vita

Sunil Prajapati was raised in Athens, Texas and graduated from Athens High School in 2013. He attended the University of Texas and graduated with a Bachelor of Science in Mechanical Engineering in May 2017. While pursuing his undergraduate degree, he was a research assistant in the Rewire research Laboratory under the direction of Dr. James Sulzer. In addition, he was an intern for the Center for Injury Biomechanics at Wake Forest University. Sunil was accepted into graduate school at the University of Texas where he chose to pursue his Master of Science in Engineering with a specialization in Biomechanics and continue his work in Dr. James Sulzer's Rewire Laboratory in August 2017.

Permanent email address: sprajapati1094@gmail.com

This dissertation was typed by the author.